Journal of Applied Polymer Science

Antimicrobial N-halamine coatings synthesized via vapor-phase assisted polymerization

Guanghui Xi, Yanlei Xiu, Lu Wang, Xiangdong Liu
College of Materials and Textiles, Zhejiang Sci-Tech University, Hangzhou Zhejiang 310018, China
Correspondence to: X. Liu (E-mail: liuxd@zstu.edu.cn)

ABSTRACT: An N-halamine monomer, 3-allyl-5,5-dimethylhydantoin (ADMH), was synthesized by a Gabriel reaction of 5,5-dimethylhydantoin and 3-bromopropene. Antimicrobial coatings of poly[1-(4,4-dimethyl-2,5-dioxoimidazolidin-1-methyl)ethylene] were prepared on plasma-treated PET fabrics via a vapor-phase assisted polymerization (VAP) process using gasified ADMH as monomer. The coatings endow the PET fabrics with an antimicrobial efficiency greater than 80% for both *Escherichia coli* and *Staphylococcus aureus* after chlorination of the N-halamine polymer with dilute bleach solution. The obtained antimicrobial effect has remarkable durability that can bear over 30 times of stringent laundering tests. Compared with other antimicrobial finishing methods, the VAP methodology offers great advantages in needless of organic solvents and small consumption of monomer. It has potential applications in a wide variety of fields such as hygienic clothing, underwear, socks, and medical textiles. © 2014 Wiley Periodicals, Inc. J. Appl. Polym. Sci. **2015**, *132*, 41824.

KEYWORDS: fibers; grafting; polyesters; surfaces and interfaces

Received 3 September 2014; accepted 30 November 2014
DOI: 10.1002/app.41824

INTRODUCTION

Antimicrobial textile provides protections not only against infectious diseases but also against odor, staining, and fiber damages caused by rotting.[1,2] A broad range of antimicrobial textile products, for example, hygienic clothing, underwear, socks, shoe linings, outdoor textiles, air filters, automotive textiles, domestic home furnishings, and medical textiles have been developed to respond the substantial demand. Generally, the antimicrobial activity of textiles results from antimicrobial agents, such as quaternary ammonium compounds,[3,4] triclosan,[5,6] polyhexamethylene biguanide (PHMB)[7,8] noble metals,[9] and metal oxides[10] (TiO_2, ZnO). Because most of the antimicrobials cannot be chemically linked to textile fibers, the antimicrobial efficiency of the leaching agents directly depends on their concentration and does not withstand repeated laundering processes. Although the antimicrobials those bound on fabric surface are much more resistant to repeated laundering in comparison to the leaching agents, antimicrobial function of the immobilized agents still decreases with adsorption of dirt or dead microorganisms. Therefore, a combination of reproducibility and immobility are favorable for expanding the antimicrobial durability of textiles. In fact, a number of studies have focused on developing novel antimicrobial agents linked on the fiber surface. For examples, chitosan,[11] quaternary ammonium compounds,[12–14] silver-carboxylate ion,[15] melamine containing polymers,[16] and N-halamines[17–22] have been reported to be efficiently antimicrobic. Among these antimicrobial agents, N-halamines are the most widely studied and best developed ones because they are active for a broad spectrum of microorganisms, having strong-stability in aqueous solutions, and can be regenerated in sodium hypochlorite solutions.

On the other hand, a number of finishing techniques have been demonstrated for linking N-halamine functional groups to various textiles. The important instances included padding, dipping, soaking, and coating methods.[18,23–29] However, these finishing processes have several limitations: (i) excessive consumption of halamine precursors, (ii) large quantity of water or organic solvents is required (unfriendly for environment), and (iii) great challenge in modifying of single-side of fabrics. In fact, the application of N-halamines was limited by the disadvantages and the resulting industrial symptoms such as high-cost, pollution, and the problems in health and safety.

Herein, we report a simple and convenient method for the fabrication of N-halamine coated textiles via vapor-phase assisted polymerization (VAP) method. VAP approach is a new way developed recently for modifying solid surfaces.[30,31] The key idea in the VAP method is that monomer is gasified and initiator is immobilized on a solid surface. It was demonstrated that the VAP process can construct a very thin polymer layer on one side surface of the substrate without solvent. Therefore, the

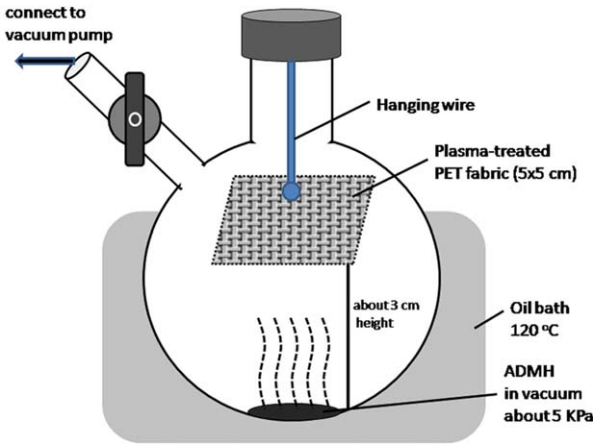

Figure 1. Schematic drawing of the experimental set used for the VAP process. [Color figure can be viewed in the online issue, which is available at wileyonlinelibrary.com.]

application of the VAP method to polymerize the N-halamine monomers is expectable for responding to the limitations troubled in the general finishing methods. In the present work, commercial PET fabrics are treated with plasma beam to generate free-radicals on the surface, and then the N-halamine monomer, 3-allyl-5, 5-dimethylhydantoin (ADMH), is gasified and graft-polymerized on the plasma-treated PET fabric surface. The resulting antimicrobial coatings on PET fabrics are subjected to structural and functional tests, that is, the surface morphology and chemical structure are investigated by SEM and FTIR, and the antimicrobial function is characterized by standard antimicrobial tests.

EXPERIMENTAL

Materials

PET fabrics used were purchased from a local fabric store (60 ends/cm, 30 picks/cm, 0.32 mm thickness). Before chemical modification, the PET fabric samples (5.0 cm × 5.0 cm) were cleaned by ultrasonic washing of deionized water (30 min × 3 times). 5,5-Dimethylhydantoin (DMH) and allyl bromide were purchased from J&K Scientific (China, ShangHai) and used without further purification. All other reagents were purchased from either Shanghai Crystal Pure Industrial or Tokyo Chemical Industry (China, ShangHai). Deionized water with a resistivity of 18.2 MΩ cm was used throughout all experiments.

Synthesis of ADMH

ADMH was synthesized by a improved method basing on a previous report.[21] KOH (2.8 g, 50 mmol) and allyl bromide (4.4 mL, 50 mmol) was added to a DMH (6.4 g, 50 mmol) solution in water (10 mL). The mixture was stirred at 60°C for 3 h and dried with a rotary-evaporator. The resulted solid was recrystallized from petroleum ether, yielding ADMH product.

Typical Procedure of VAP Polymerization on the PET Fabric Surface

The PET fabric was pretreated with a plasma generator (CTP-2000K, China) in atmosphere (60 V, 45 s), and hanged over ADMH monomer (0.17 g, 1.0 mmol) in a flask (Figure 1). The vacuum pressure in the flask was reduced to 5 KPa and then sealed. The monomer was heated at 120°C under vacuum condition to generate ADMH vapor until the VAP process was finished. The resulting PET fabric surface was immersed to a NaClO solution (5 wt %, pH 4) with stirring for 1 h, rinsing with water (100 mL × 3 times), and drying under vacuum to give the chloridized PET fabric. Other optimization experiments were designed as shown in Table I.

Material Characterizations

Surface morphology was investigated by utilizing JSM-6700F field emission scanning electron microscope (FE-SEM, JEOL, Japan) after gold coating (thickness of approximately 10 nm). 1H-NMR spectrum was recorded on a Bruker AVANCE AV (400 MHz) spectrometer. Fourier transform infrared (FTIR) measurements were performed on a Nicolet Avatar 370 spectrometer in a normal transmission mode. Attenuated total reflectance infrared (ATR-IR) spectra were collected using a Nicolet Avatar 370 spectrophotometer equipped with an ATR accessory. Mechanical tests were carried out on an electronic fabric tensile tester (YG065, China). The fabric samples were cut to rectangle shape (50 × 200 mm^2) and were stretched at a rate of 200 mm/min. The average data were taken from three

Table I. Experimental Factors for the Plasma and VAP Treatments

Runs	Plasma time (s)	Plasma voltage (V)	VAP temperature (°C)	VAP time (h)	Resulting fabric color	Resulting fabric ATR-IR peak at 2850 cm^{-1}
Control	-	-	-	-	White	Unclear
1	60	60	-	-	White	Unclear
2	60	90	-	-	Lightly brown	Unclear
3	30	60	120	2	White	Unclear
4	45	60	120	2	White	Clear
5	60	60	120	2	White	Clear
6	60	30	120	2	White	Unclear
7	60	60	100	2	White	Unclear
8	45	60	120	0.5	White	Unclear
9	45	60	120	1	White	Clear

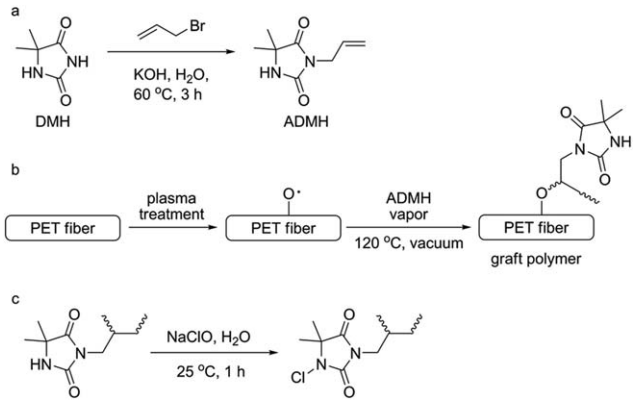

Figure 2. Schemes of (a) the synthesis of ADMH, (b) the VAP process on the PET fiber surface, and (c) the chloridization of the N-halamine moieties in the graft polymer.

repeat tests. Vapor transmission rates of the modified PET fabrics were measured using an ASTME-96 (open cup test) method. In a typical example, a PET fabric sample is placed tightly over a cup of water. The vapor transmission rate is calculated by measuring the weight loss of water in the cup over 24 h. The calculated formula as follow:

$$T(\mathrm{g/m^2/d}) = \frac{m_o - m_a}{\pi r^2} \quad (1)$$

Where T is the vapor transmission rate ($\mathrm{g/m^2/d}$), which means the lost weight on per square meter one day. m_o *and* m_a are the original water mass and the water mass remained after 24 h, respectively, and r is the inside radius of the cup. The vapor transmission rate was the average taken from three repeat tests.

Antimicrobial Test

Escherichia coli (*E. coli*, ATCC 1555) and *Staphylococcus aureus* (*S. aureus*, ATCC 547) were used as model microorganisms for the antimicrobial tests. Both modified and unmodified PET fabric samples were challenged with bacteria using an improved AATCC test method 100–1999 for antimicrobial efficacy testing. Before each assay, the test bacteria were incubated in Letheen broth (LB) fluid nutrient medium (containing 5 g/L yeast extract, 10 g/L peptone, 10 g/L NaCl and adjust pH to 7.4) at 37°C for 24 h. A standardized density of bacteria was used for the challenge inoculation. The fabric specimens (0.05 g) were cut to about 5 mm pieces, sterilized by UV light for 30 min, placed in a sterile container. 5.0 μL of activated *E. coli* or *S. aureus* in 4 mL fluid nutrient medium (108 CFU/mL) was added into sterile tubes containing modified PET fabrics, shaken at 25°C for 18 h at 150 rpm. The supernatant was diluted to an appropriate concentration, dispersed onto LB agar plants, and incubated at 37°C for 24 h. The number of survival microorganism was determined by counting the colonies as a colony-forming unit (CFU)/mL, and bacteriostatic reduction rate of microorganisms was calculated as follows:

$$R = \frac{(B-A)}{B} \times 100 \quad (2)$$

where R is the bacteriostatic reduction rate, A and B are the (CFU)/mL of surviving microorganisms after 18 h for the agar plate containing test sample and the blank sample (inoculum only), respectively.

Laundering Durability Test

The laundering durability was evaluated by repeating a stringent washing-cycle and monitoring the antimicrobial efficacy of the modified samples. The fabrics (15 × 15 $\mathrm{mm^2}$) were washed by 50 mL of an aqueous solution of sodium dodecanesulfonate (2.0%, w/w) in a beaker (diameter, 50 mm) with stirring (300 rpm, magnetic stirrer, 9 × 25 $\mathrm{mm^2}$) at 25°C for 10 min, rinsed with deionized water (10 mL × 4 times), and dried at 60°C. The antibacterial activity of the laundered sample was examined using the same inhibition test as described above.

RESULTS AND DISCUSSION

Chemical Structure Analysis

ADMH monomer was synthesized by Gabriel reaction of DMH and allyl bromide in an alkaline condition as shown in Figure 2.

Figure 3(left) shows the ^{1}H-NMR spectrum of the synthesized ADMH. The peak at 6.31 ppm is attributable to the secondary amine, while the peaks at 5.58 ppm and 5.18 ppm are assignable to the protons in the C═C bond. The peaks appeared at 4.11 ppm and 1.45 ppm are believed due to the methylene and methyl groups, respectively. The integral ratio of the five peaks was 1 : 1 : 2 : 2 : 6, which is in good consistent with the 12

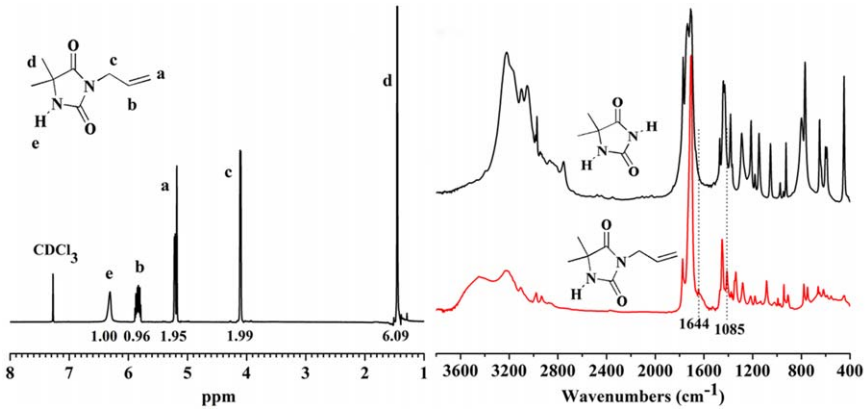

Figure 3. ^{1}H-NMR spectrum of ADMH (left) and FTIR spectra of DMH and ADMH (right). [Color figure can be viewed in the online issue, which is available at wileyonlinelibrary.com.]

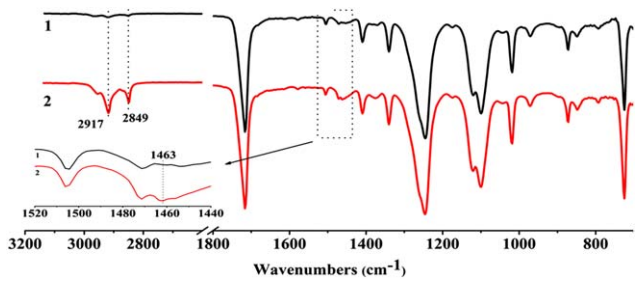

Figure 4. ATR-IR spectra of (1) the pristine PET fabric surface and (2) the VAP modified PET fabric surface. [Color figure can be viewed in the online issue, which is available at wileyonlinelibrary.com.]

protons in ADMH structural formula. Figure 3(right) shows the FTIR spectra of ADMH and its reactant, DMH. The peak newly appeared at 1085 cm^{-1} in ADMH's spectrum is attributable to the C—N stretching vibration. The peak at 1644 cm^{-1} responds to the stretching vibrations of the C═C bond, while the peaks appeared at 909 cm^{-1} and 992 cm^{-1} are assignable to the plane bending vibration.

The PET fabric was pretreated by a plasma beam in atmosphere to break the covalent bonds and generate radicals on the surface. It was well known that a plasma treatment can only alter the surface, but remain the bulk properties of the substrate. Most vinyl monomers can be graft-polymerized on the activated surface having radicals induced by plasma treatments.[32,33]

In this study, a graft-polymerization on the plasma-treated PET fabrics was performed using vaporized ADMH monomer to achieve a solventless surface modification [Figure 2(b)]. This process resulted in an antimicrobial polymer, poly[1-(4,4-dimethyl-2,5-dioxoimidazolidin-1-methyl)ethylene], grafted on the surface of the PET fabrics.

Figure 4 compares the ATR-IR spectra of the original PET fabric (1) and the VAP modified PET fabric (2). The PET structure was verified by the characteristic peak at 1712 cm^{-1}, which

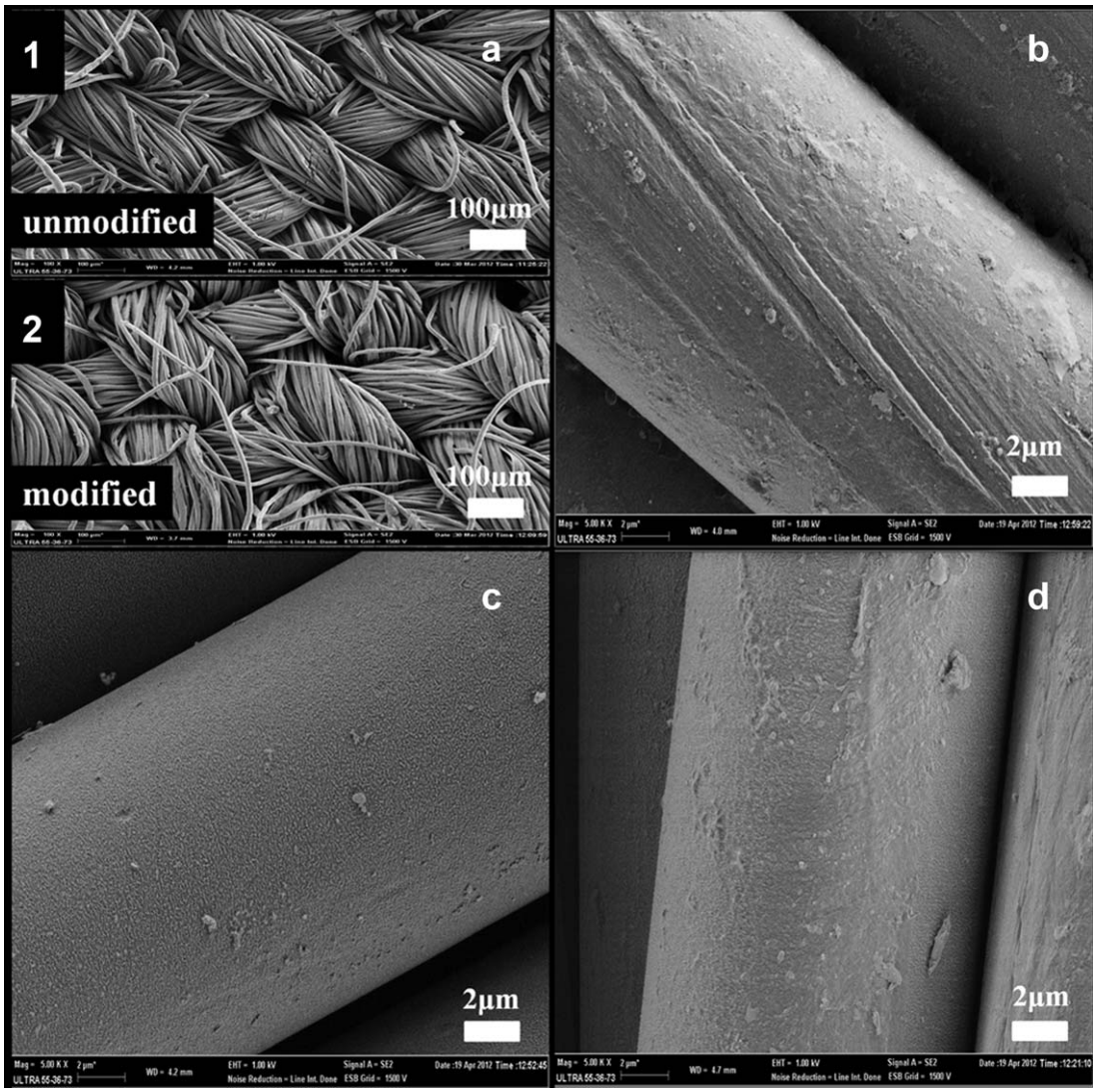

Figure 5. Low magnification SEM images of pristine PET fibers (a1) and VAP modified PET fibers (a2); high magnification SEM images of pristine PET fiber (b), plasma-treated PET fiber (c), and VAP modified PET fiber (d).

Table II. Antibacterial Effect Against *E. coli*[a] and *S. aureus*[b]

PET sample	VAP time (h)	Bacterial reduction rate (%)	
		E. coli	*S. aureus*
Control	0	37.3 ± 1.2[c]	48.3 ± 1.5
PET1	1.0	54.4 ± 1.0	62.9 ± 0.5
PET2	1.5	66.3 ± 1.1	74.4 ± 0.9
PET3	2.0	78.0 ± 3.5	84.9 ± 0.2
PET4	2.5	80.4 ± 2.8	83.2 ± 0.8

[a] The inoculum population was 8.12×10^7 cfu/sample.
[b] The inoculum population was 7.66×10^7 cfu/sample.
[c] The mean ± SD, the average values were obtained from three tests.

could be attributed to the C═O groups. While the absorption peaks appeared at 2917, 2849, and 1463 cm^{-1} can be assigned to the methyl group of the ADMH. This result suggests that the N-halamine structure has been introduced to the PET fabric surface.

To optimize the experimental factors such as plasma voltage, plasma treatment time, VAP temperature and VAP time, we designed optimization experiments as shown in Table I. The fabric color and the ATR-IR peak at 1850 cm^{-1}, which are associated to the substrate damage and quantity of polymerized ADMH, respectively, were used as the index for the treatment evaluation. For the plasma treatment, voltage of 60 V and treatment time of 45 s was suitable to avoid excessive damage on the PET substrates. On the other hand, vacuum pressure, heating temperature, and the polymerization time are the important factors in the VAP process. By fixing the initial vacuum pressure at 5 KPa, it was found that the condition of 120°C and 1 h is enough to make considerable polymeric coating.

SEM Morphological Observations

Figure 5 shows the SEM images of the unmodified PET fabric, the plasma-treated PET fabric, and the product sample obtained after the VAP modifying process. The comparative pair of the low magnification SEM images of the pristine PET fabric [Figure 5(a1)] and the modified sample after whole VAP process [Figure 5(a2)] reveals that there are no obvious differences between the original and modified fiber surfaces. However, it was observed from the SEM images obtained at higher magnification [Figure 5(b–d)] that the surface of the plasma-treated [Figure 5(c)] and the VAP modified fibers [Figure 5(d)] became rougher in comparison with the original fibers in nanoscale [Figure 5(b)]. Comparably, numerous protrusions and horizontal channels-like structures were developed on the plasma-treated surface. Otherwise, an even distribution of incontinuous network structures appeared on the fiber surface after the polymerization of ADMH. This result means that the modified surface was slightly covered by the N-halamine polymer when the finishing process was finished.

In addition, weight change of the PET fabrics (3×3 cm^2) after the polymerization was not measurable by a precise balance (0.1 mg accuracy), indicating that only a small quantity of the polymer has linked to the PET fabric surface (less than 0.2 wt %). Because the VAP process undergoes in a vapor phase of the monomer, monomer concentration must be much lower than that in bulk polymerizations or in solution polymerizations. The low monomer concentration should result in a very slow polymerization rate, which is often of an advantaged point for surface modification as monomer consumption can be easy controlled.

Antibacterial Efficacy

After chlorination of the polymer grafted on the PET fabric surface, we investigated the antimicrobial efficacy of the modified fabric. The gram-positive *S. aureus* (ATCC 6538) and the gram-negative *E. coli* (ATCC 35218) were used as test microorganisms because they are the major cause of cross-infection in hospitals. The biocidal efficacy data for both original and modified PET fabrics are presented in Table II and Figure 6.

The original PET fabric shows bacteriostatic reduction rates of 37.3% and 48.3% for *E. coli* and *S. aureus*, respectively. As shown in Figure 6, the antimicrobial efficacy for both testing microorganisms increases linearly with increasing the polymerization time, and reaches the maximum antimicrobial rate about 80% at 2 h. With further increasing VAP time more than two hours, the data for both test microorganisms become almost constant around 80%. This bacteriostatic reduction rate is close to that of the antimicrobial coatings of N-halamine and other reagent reported recently.[22,34] N-halamines have been well known to be effective toward a broad spectrum of microorganisms. Stable N-halamines inactivate microorganisms through direct transfer of the oxidative halogen to the cell membrane leading to cell death.[35] As exceeding NaClO dosage was used in the chlorination process, the antimicrobial efficacy of the modified PET samples directly depend on the quantity of the N-halamine groups linked on the PET surface. When the fiber surface was fully covered by the N-halamine polymer, exceeding polymerization will not further enhance the antimicrobial efficacy.

Laundering Durability

The antibacterial effect of N-halamine polymers is regenerative due to the oxidative halogen on the surface can be recharged by exposure to dilute household bleach. However, there is a

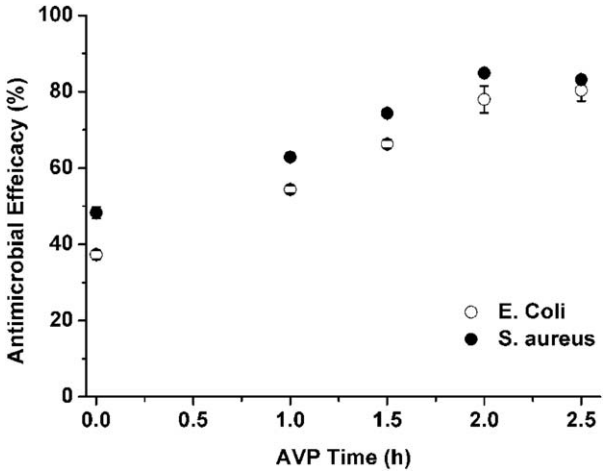

Figure 6. Influence of VAP time on antimicrobial ability of the VAP modified PET fabric.

Table III. The Washing Durability of the N-Halamine Modified PET Fabric

PET sample	Laundering cycles	Bacterial reduction rate (%)	
		E. coli	*S. aureus*
PET3	0	78.0 ± 3.5[a]	84.9 ± 0.2
PET3	10	76.8 ± 5.1	77.1 ± 4.9
PET3	20	71.9 ± 4.6	73.5 ± 3.4
PET3	30	65.1 ± 3.7	69.7 ± 4.3

[a] The mean ± SD, the average values were obtained from three tests.

durability problem to the antimicrobial textiles because of the disconnection of the covalent bonds between the N-halamine molecules and the textile during the washing processes.

In this study, we used a stringent washing test to estimate the washing durability of the N-halamine modified PET fabrics. The results were shown in Table III. For the modified PET fabrics, they were chlorinated after 10, 20, and 30 washing cycles. Even after 30 washing cycles, bacteriostatic reduction rates of the modified PET fabric are 65.1% and 69.7% for *E. coli* and *S. aureus*, respectively. This means that the N-halamine modified fabrics still are biocidal effective. The minor loss of antimicrobial efficacy after 30 laundering cycles could be contributed to the departure of the N-halamine moieties from the PET fabrics.

Mechanical Property

As shown in Figure 7, the pristine PET fabric (50 × 200 mm^2) has a good mechanical property. Its breaking strength reached to 492 N. The plasma treated PET fabric was lightly weakened by the plasma treatment. The breaking strength of the plasma treated PET fabrics decreased to 471 N. The damage by the plasma treatment can be partially repaired by the polymeric coating produced by the VAP process. Figure 7 shows that the breaking strength of the VAP modified fabrics increases with increase of VAP time, and retunes to 491 N after 2.5 h VAP modification. This breaking tensile strength is much close to the pristine PET fabric samples.

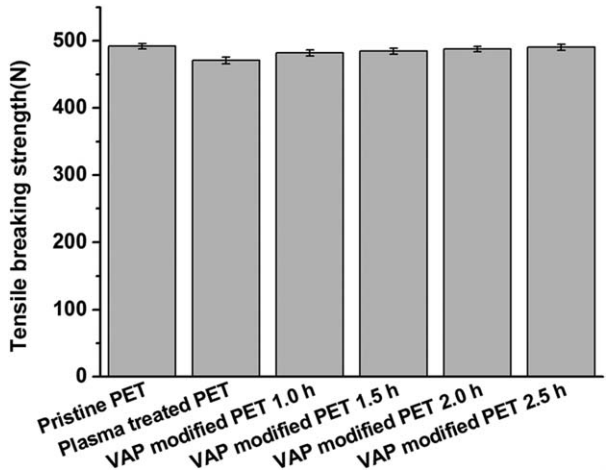

Figure 7. Mechanical properties of pristine PET and the modified PET fabrics.

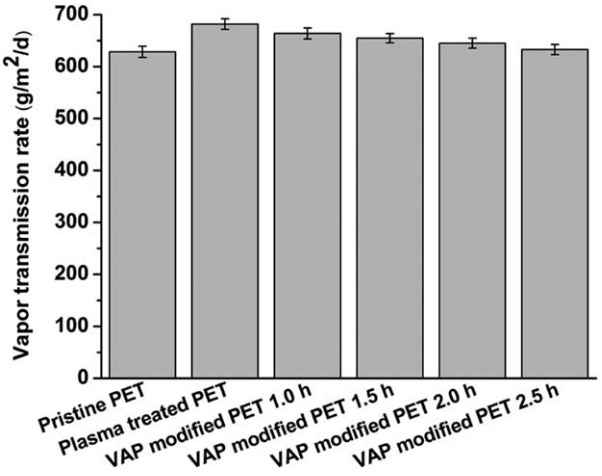

Figure 8. Water vapor transmission rates of pristine PET and the modified PET fabrics.

Vapor Transmission Property

Figure 8 shows the vapor transmission rates of the modified PET fabrics. They are averaged from three tests, which were all performed at 25°C and 50% RH for 1 day. The plasma treated PET fabric showed a good vapor transmission rate of 681.7 g/m^2, which is slightly better than that of the pristine PET fabric (628.2 g/m^2). The modified PET fabric with a VAP treatment for 2.5 h has a vapor transmission rate of 632.6 g/m^2, which is very similar to that of the pristine PET fabric. These results may be explained by the fact that the plasma treatment results in hydrophilic surface damage on the PET substrate but the subsequent VAP process partially repairs them. In a total result, the modified PET fabric through the whole VAP process has only a little change in vapor transmission property by contrast with the original PET fabric.

CONCLUSIONS

N-halamine monomer, 3-allyl-5,5-dimethylhydantoin (ADMH), was synthesized by a Gabriel reaction of 5,5-dimethylhydantoin and 3-bromopropene. Antimicrobial PET fabrics were fabricated via graft-polymerization in vapor phase of the ADMH monomer, and the polymeric coating was confirmed by ATR-IR and XPS analyses. After chlorination, the modified PET fabrics exhibited antibacterial effect for both microorganisms of *S. aureus* and *E. coli* greater than 80%, and showed a remarkable antibacterial durability that can bear over 30 times of stringent laundering tests. Because of the advantages of needless of organic solvents and small quantity of consumption of monomer, the VAP process of the N-halamine monomer has great potential for practical applications in biomedical textiles.

ACKNOWLEDGMENTS

This work was financially supported by the Natural Science Foundation of Zhejiang Province (LY12E03007), the Scientific Research Foundation for the Returned Overseas Chinese Scholars, the State Education Ministry (1101603-C).

REFERENCES

1. Gao, Y.; Cranston, R. *Text. Res. J.* **2008**, *78*, 60.

2. Simoncic, B.; Tomsic, B. *Text. Res. J.* **2010**, *80*, 1721.
3. Lu, G.; Wu, D.; Fu, R. *React. Funct. Polym.* **2007**, *67*, 355.
4. Marini, M.; Bondi, M.; Iseppi, R.; Toselli, M.; Pilati, F. *Eur. Polym. J.* **2007**, *43*, 3621.
5. Orhan, M.; Kut, D.; Gunesoglu, C. *Indian J. Fiber Text. Res.* **2007**, *32*, 114.
6. Windler, L.; Height, M.; Nowack, B. *Environ. Int.* **2013**, *53*, 62.
7. Gao, Y.; Cranston, R. *J. Appl. Polym. Sci.* **2010**, *117*, 3075.
8. Kawabata, A.; Taylor, J. A. *Carbohydr. Polym.* **2007**, *67*, 375.
9. Montazer, M.; Hajimirzababa, H.; Rahimi, M. K.; Alibakhshi, S. *Fibre Text. E. Eur.* **2012**, *20*, 96.
10. Lam, Y. L.; Kan, C. W.; Yuen, C. W. M. *Fiber Polym.* **2013**, *14*, 52.
11. Lim, S. H.; Hudson, S. M. *Carbohydr. Polym.* **2004**, *56*, 227.
12. Diz, M.; Jocić, D.; Infante, M.; Erra, P. *Text. Res. J.* **1997**, *67*, 486.
13. Ozer, R. R.; Hill, W. C.; Rogers, M. E.; Evans, M. *J. Appl. Polym. Sci.* **2010**, *118*, 2397.
14. Chen, S.; Chen, S.; Jiang, S.; Xiong, M.; Luo, J.; Tang, J.; Ge, Z. *ASC Appl. Mater. Interface* **2011**, *3*, 1154.
15. Parikh, D. V.; Edwards, J. V.; Condon, B. D.; Parikh, A. D. *AATCC Rev.* **2008**, *8*, 38.
16. Zhu, J.; Bahramian, Q.; Gibson, P.; Schreuder, G. H.; Sun, G. *J. Mater. Chem.* **2012**, *22*, 8532.
17. Jiang, Z. M.; Ma, K. K.; Du, J. M.; Li, R.; Ren, X. H.; Huang, T. S. *Appl. Surf. Sci.* **2014**, *288*, 518.
18. Zhang, B.; Jiao, Y. C.; Kang, Z. Z.; Ma, K. K.; Ren, X. H.; Liang, J. *Cellulose* **2013**, *20*, 3067.
19. Cerkez, I.; Kocer, H. B.; Worley, S. D.; Broughton, R. M.; Huang, T. S. *React. Funct. Polym.* **2012**, *72*, 673.
20. Hui, F.; Debiemme-Chouvy, C. *Biomacromolecules* **2013**, *14*, 585.
21. Sun, Y.; Sun, G. *J. Appl. Polym. Sci.* **2001**, *80*, 2460.
22. Li, R.; Sun, M.; Jiang, Z.; Ren, X.; Huang, T. S. *Fiber Polym.* **2014**, *15*, 234.
23. Liang, J.; Chen, Y.; Ren, X.; Wu, R.; Barnes, K.; Worley, S. D.; Broughton, R. M.; Cho, U.; Kocer, H.; Huang, T. S. *Ind. Eng. Chem. Res.* **2007**, *46*, 6425.
24. Cerkez, I.; Worley, S. D.; Broughton, R. M.; Huang, T. S. *React. Funct. Polym.* **2013**, *73*, 1412.
25. Liang, J.; Chen, Y.; Barnes, K.; Wu, R.; Worley, S. D.; Huang, T. S. *Biomaterials* **2006**, *27*, 2495.
26. Ren, X.; Kou, L.; Liang, J.; Worley, S. D.; Tzou, Y. M.; Huang, T. S. *Cellulose* **2008**, *15*, 593.
27. Liu, Y.; Liu, Y.; Ren, X.; Huang, T. S. *Appl. Surf. Sci.* **2014**, *296*, 231.
28. Kim, S. S.; Ryoo, K. Y.; Lim, J.; Seo, B.; Lee, J. *Fiber Polym.* **2013**, *14*, 409.
29. Cerkez, I.; Worley, S. D.; Broughton, R. M.; Huang, T. S. *Prog. Org. Coat.* **2013**, *76*, 1082.
30. Andou, Y.; Jeong, J. M.; Hiki, S.; Nishida, H.; Endo, T. *Macromolecules* **2009**, *42*, 768.
31. Andou, Y.; Jeong, J. M.; Nishida, H.; Endo, T. *Macromolecules* **2009**, *42*, 7930.
32. Johnson, D.; Osada, Y.; Bell, A.; Shen, M. *Macromolecules* **1981**, *14*, 118.
33. Chen, K. S.; Ku, Y. A.; Lin, H. R.; Yan, T. R.; Sheu, D. C.; Chen, T. M. *J. Appl. Polym. Sci.* **2006**, *100*, 803.
34. Han, S.; Yang, Y. *Dyes Pigments* **2005**, *64*, 157.
35. Denyer, S. P. *Int. Biodeter. Biodegrad.* **1995**, *36*, 227.